



**HAL**  
open science

## Combination of the Wenner resistivimeter and Torrent permeameter methods for assessing carbonation depth and saturation level of concrete

Stéphanie Bonnet, Jean-Paul Balayssac

► **To cite this version:**

Stéphanie Bonnet, Jean-Paul Balayssac. Combination of the Wenner resistivimeter and Torrent permeameter methods for assessing carbonation depth and saturation level of concrete. *Construction and Building Materials*, 2018, 188, pp.1149-1165. 10.1016/j.conbuildmat.2018.07.151 . hal-01917049

**HAL Id: hal-01917049**

**<https://hal.insa-toulouse.fr/hal-01917049>**

Submitted on 26 Nov 2018

**HAL** is a multi-disciplinary open access archive for the deposit and dissemination of scientific research documents, whether they are published or not. The documents may come from teaching and research institutions in France or abroad, or from public or private research centers.

L'archive ouverte pluridisciplinaire **HAL**, est destinée au dépôt et à la diffusion de documents scientifiques de niveau recherche, publiés ou non, émanant des établissements d'enseignement et de recherche français ou étrangers, des laboratoires publics ou privés.

1                   **Combination of the Wenner resistivity meter and Torrent Permeameter methods for**  
2                   **assessing carbonation depth and saturation level of concrete**

3  
4  
5                   Stéphanie BONNET<sup>1</sup>, Jean-Paul BALAYSSAC<sup>2</sup>

6  
7                   <sup>1</sup> LUNAM Université, Université de Nantes, GeM, Institut de Recherche en Génie civil et  
8                   Mécanique – CNRS UMR 6183 52 rue Michel Ange, BP 420, 44606 Saint-Nazaire cedex,  
9                   France  
10                  stephanie.bonnet@univ-nantes.fr

11  
12                  <sup>2</sup> LMDC, INSA/UPS Génie Civil, 135 Avenue de Rangueil, 31077 Toulouse cedex 04 France  
13                  jean-paul.balayssac@insa-toulouse.fr

14  
15                  Abstract

16                  Assessing carbonation depth is of great interest for the diagnosis of reinforced concrete  
17                  structures because carbonation is one of the origins of steel corrosion. The assessment of  
18                  carbonation depth is usually performed by a simple and reliable semi-destructive test  
19                  consisting in spraying a colored indicator on a sample extracted from the structure. When the  
20                  structure is large, this test must be reproduced many times if an assessment of the variability  
21                  of carbonation depth is required. In this case, the extraction of multiple samples can be  
22                  prohibitive from the technical and economic points of view. So, in this case, a non-destructive  
23                  testing (NDT) method could be relevant. However, even when NDT methods can be used,  
24                  there is a need to improve the interpretation of their results. In this study, the use of two usual  
25                  NDT methods is proposed: resistivity measurement by a Wenner probe and surface  
26                  permeability assessment by a Torrent permeameter. Both techniques are implemented on  
27                  carbonated slabs having different carbonated depths and at different saturation degrees. The  
28                  results show that the two techniques are sensitive to moisture and carbonation. For a given  
29                  saturation level, resistivity increases when the carbonated depth increases and resistivity  
30                  decreases when the saturation level increases. Torrent permeability decreases when the  
31                  saturation degree and carbonated depth increase. Good repeatability is observed for resistivity  
32                  measurements while a larger scatter is obtained for Torrent permeability. Empirical laws are

<sup>1</sup> Corresponding author. Tel.: +33 2 40 17 81 88;  
E-mail address: stephanie.bonnet@univ-nantes.fr

33 built for the relationships between resistivity or permeability and saturation degree and  
34 carbonated depth. For resistivity, either a linear model between resistivity and saturation  
35 degree is used or Archie's law is adapted to take the effect of carbonation into account.  
36 Following the same idea, a linear law between Torrent permeability and saturation degree is  
37 adapted to the effect of carbonation. Because resistivity can be measured only if the saturation  
38 degree is rather high, i.e. if there is a continuity of the interstitial solution, and because  
39 permeability assessment is impossible if the concrete is fully saturated, these laws are limited  
40 to saturation degrees in the 40 to 83% range.

41 Then, these laws are used to predict carbonation depth and saturation degree on a wall  
42 designed with the same concrete but stored in different conditions. The results show that  
43 resistivity and Torrent permeability can be used for the combined assessment of carbonation  
44 depth and saturation degree in laboratory conditions.

45 Keywords: Concrete, carbonation depth, saturation level, Torrent permeability, Wenner  
46 resistivity

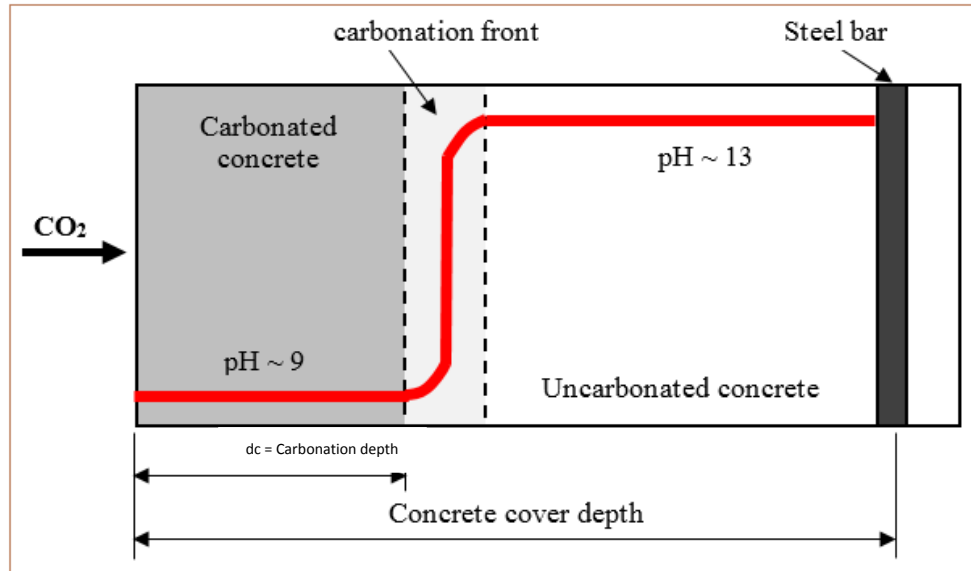
47

## 48 1 Introduction

49 The corrosion of reinforcing steel within reinforced concrete structures produces damage such  
50 as spalling of the concrete cover. Steel parts then remain uncovered and cause a sharp  
51 decrease in the load-bearing capacity of the structure. This failure condition is usually due to  
52 the presence of chloride or to a carbonation process. The present study was conducted to  
53 examine, more specifically, the carbonation process. Carbonation is a physical-chemical  
54 process, which may cause a decrease in concrete pH value from 13 to 9. Carbon dioxide from  
55 the air ( $\text{CO}_2$ ) reacts with the portlandite of concrete ( $\text{Ca}(\text{OH})_2$ ) to form calcium carbonate  
56 ( $\text{CaCO}_3 + \text{H}_2\text{O}$ ) (Figure 1). If the whole of the concrete cover is carbonated, steel frame de-

57 passivation is initiated and results in the delamination of the concrete cover due to swelling of  
58 the corroded steel.

59



60

61 *Figure 1: pH decrease in concrete cover due to carbonation [Ta 2016]*

62 According to a literature review conducted by Ta *et al.* [Ta 2016 and 2018], a considerable  
63 amount of effort has been devoted to the study of the propagation of CO<sub>2</sub> and to the  
64 examination of the factors affecting the carbonation rate, such as mix proportions in concrete  
65 (e.g., cement content and water to cement ratio) [Chang 2004], [Papadakis 1989], mineral  
66 admixtures [Hui-Sheng 2009] [Papadakis, 1999 and 2000] [Younsi 2011], exposure  
67 conditions (e.g., temperature (T) [Saetta 1993] and external relative humidity (RH) [Houst  
68 1983] [Papadakis, 1989]).

69 Because carbonation takes place throughout the life cycle of concrete, accurate assessment of  
70 its progress is essential to predict the initiation of steel corrosion. To achieve this, the  
71 condition of the concrete cover of structures must be surveyed at regular intervals in order to  
72 plan maintenance. The most common technique used for measuring carbonation depth is the  
73 semi-destructive coring method [RILEM CPC-18]. Phenolphthalein is sprayed on the fresh  
74 cores obtained [Chang 2006, Villain 2006]. Phenolphthalein is an organic compound used as a

75 pH indicator: it is colorless at low pH values (around pH 9) but has a characteristic purple or  
76 magenta color at pH values exceeding 10.5.

77 Testing is carried out at structure level with a sufficiently representative number of  
78 measurement points, requiring a large variety of core samples [Breysse, 2017]. For improved  
79 conservation of structures, non-destructive survey techniques must be favored as they can be  
80 used to detect and characterize defects or damage without the need for coring [Bungey 2006].

81 The objective of this research is to examine the sensitivity to the presence of carbonation in  
82 concrete structures of two currently available non-destructive methods: the Torrent  
83 permeameter and the Wenner resistivimeter. Carbonation affects the microstructure of  
84 concrete by reducing porosity [Nagla 1997, Auroy 2015] because the volume of hydrates  
85 increases by an average of 11.7% [Song and Kwon 2007]. As the carbonation front  
86 progresses, an increasing number of pores become clogged and reduce porosity in the depth of  
87 carbonated concrete. [Porosity is one factor among others \(e.g. water content and rebars\)](#)  
88 [affecting resistivity measurements in cementitious materials](#). Sbartai et al. [Sbartai 2007] have  
89 demonstrated that resistivity increases when the W/C ratio of the studied concrete decreases,  
90 leading to decreased porosity. A similar trend was observed by Lübeck et al. [Lübeck 2012]  
91 after measuring concrete specimens with different water to binder ratios. As regards  
92 permeability, some studies addressing the problem of permeability measurements using the  
93 Cembureau method have shown that permeability decreases with the porosity of the studied  
94 concrete [Hui-Sheng 2009] [Djerbi 2008 and 2013]. This trend is also reflected by  
95 permeability measurements performed using the Torrent permeameter: Romer has measured  
96 greater permeability values in mortars with a W/C ratio of 0.6 than in mortars with a W/C  
97 ratio of 0.35 [Romer 2005] and the same tendency was also found by Neves [et al.](#) [Neves  
98 2012]. The results presented by Neves [et al.](#) show that the permeability values obtained using  
99 the Torrent method decrease as compressive strength rises and that porosity therefore

100 decreases [Neves 2015]. Sena da Fonseca *et al.* found a relation between Torrent air-  
101 permeability and open porosity measured on stones [Sena da Fonseca 2015]. So it can be  
102 assumed that the permeability of carbonated concrete is bound to decrease and that,  
103 conversely, its resistivity may increase. We therefore selected two already available non-  
104 destructive methods: the Wenner resistivimeter [Polder 2001] used to measure concrete  
105 resistivity and the Torrent permeameter [Torrent, 1992] used to measure surface permeability.  
106 In situ measurements were carried out on structures that were never completely dry for  
107 auscultation. Depending on the weather conditions, the saturation *degree* of concrete may  
108 differ. Because resistivity and permeability are both sensitive to concrete moisture content,  
109 the sensitivity must be taken into account in the measurement analysis of both devices. The  
110 influence of the resistivity as a function of the saturation level has been investigated by  
111 Sbartai *et al.* [Sbartai 2007] and the results demonstrate that concrete electrical resistivity  
112 decreases when saturation level increases. Resistivity varies between 54 and 960  $\Omega\cdot\text{m}$  but  
113 cannot be measured when the saturation level is less than 60%. Similar results are found in  
114 other studies. In [Saleem 1996], resistivity ranges from 80 to 780  $\Omega\cdot\text{m}$  and, the lower the  
115 water content, the higher the resistivity. At a mass water content of about 1.5%, the resistivity  
116 cannot be measured because the concrete slab is too dry to allow the current to flow within the  
117 sample. The work of Lopez and Gonzalez [Lopez and Gonzalez, 1993] underlines the effect  
118 of the pore saturation level in relation to resistivity. They carried out tests on mortars with a  
119 W/C ratio of 0.5. The resistivity values changed within a narrow range when the pore  
120 saturation level varied between 60 and 100%. Then, between 60 and 30%, the resistivity  
121 increased sharply, up to a limit corresponding to a saturation level at which measurement was  
122 impossible. Recent studies have improved the resistivity techniques to monitor water and  
123 chloride ingress in concrete by using a multi electrode resistivity system [Du Ploy 2015,  
124 Lecieux 2015, Fares 2018].

125 Gas permeability is a transport property characterizing [gas flow under a pressure gradient](#) and  
126 is used to determine the speed with which a gas (potentially an aggressive gas like carbon  
127 dioxide) may penetrate into concrete. Air permeability is affected by the concrete moisture  
128 content and the concrete saturation level has been shown to have an effect on transport  
129 properties. For instance, the air permeability of a concrete specimen, measured using the  
130 Cembureau method, increases when the saturation level decreases [Villain 2001, Picandet  
131 2001]. Kameche et al. [Kameche 2014] confirmed this influence [and the present study](#) was  
132 conducted to examine the intrinsic permeability variations of CEM II concrete materials  
133 according to the degree of saturation, from a saturated state to a completely dry state. Because  
134 gas intrinsic permeability decreases when the saturation level increases, Cembureau  
135 measurements are not possible with saturation rates above 80%. Romer conducted an  
136 experimental study to assess the Torrent and Cembureau methods in CEM I mortar samples  
137 prepared with different cement contents [Romer, 2005]. The tests were carried out by varying  
138 the relative humidity of the samples via processing at different ambient conditions. The  
139 results thus obtained confirm that the permeability values measured using both Cembureau  
140 and Torrent methods increase as the samples become drier. However, the study does not  
141 determine the sample saturation level.

142 It thus appears from the studies listed above that both resistivity and permeability decrease  
143 when the saturation level increases. Moreover, resistivity measurements are possible with  
144 saturation rates above 30% (water content higher than 1.5%) whereas Cembureau  
145 permeability measurements are only possible with rates below 80%.

146 Permeability is a transport property depending on the porosity of the material studied.  
147 Because carbonation decreases porosity, the surface permeability of carbonated concrete  
148 measured using the Torrent permeameter can be expected to change. As regards water  
149 permeability, the water flow is weaker in carbonated than in non-carbonated concrete [Song

150 and Kwon, 2007]. Auroy *et al.* underline a decrease in intrinsic permeability after carbonation  
151 for CEM I Portland cement [Auroy, 2015].

152 Similarly, because resistivity is affected by the material microstructure, variations in  
153 resistivity can be expected according to the carbonation depth. However, the literature  
154 reviewed for this paper contains no research on the resistivity and permeability of carbonated  
155 concrete specimens using Wenner's and Torrent's methods. The present study, therefore,  
156 addresses *carbonation and moisture* effects on resistivity and permeability measurements in  
157 terms of both quality and quantity *in laboratory conditions*. *It is also important to note that*  
158 *rebar close to surface affects the resistivity*. *We chose to avoid this effect as it is difficult to*  
159 *evaluate, except maybe by using a numerical model for the determination of apparent*  
160 *resistivity* [Nguyen 2017].

161 Using the Wenner resistivimeter and the Torrent permeameter, and taking account of the  
162 sensitivity of the measurement equipment, resistivity and permeability results measured in  
163 concrete slabs made of the same mixture, with varying carbonation depths and saturation  
164 levels ranging from a dry state to a saturated state, were determined. The experimental results  
165 are analyzed below and translated into laws considering the dispersion of the measurement  
166 values. The objective of this analysis is the simultaneous use of both non-destructive methods  
167 (NDT) to *assess* saturation level and carbonation depth in real structures. Finally, the laws of  
168 correlation established were validated using a concrete wall made of the same concrete mix as  
169 the experimental slabs.

170

171

172

173

174



175        2    Materials and experimental program

176        2.1   Concrete specimens

177    The concrete mix was composed of CPA-CEM I 52.5 Portland cement with a water/cement  
178    ratio of 0.8 to accelerate the carbonation process (Table 1). Eleven slabs (rectangles 50 x 25  
179    and 12 cm thick) were prepared from a single batch of concrete in a laboratory in Toulouse  
180    (France): nine were cast for non-destructive testing, one was used for determining the  
181    physical and mechanical properties and the last one was sealed on five faces and put into the  
182    carbonation chamber to monitor carbonation depth. The concrete mixtures were cast in plastic  
183    molds and compacted under vibration. After casting, the slabs were stored in a room at 20 °C  
184    with about 95% relative humidity (RH) for 24 h until demolding, after which they were cured  
185    in water at 20 °C for 28 days.

186    *After 28 days, two slabs were used to assess the mechanical and physical properties of the*  
187    *concrete. Cylindrical cores were extracted from these slabs to drive these tests.* The results are  
188    summarized in Tables 2 and 3. Open porosity was measured using the water saturation  
189    method on three specimens. Three specimens were tested under axial compressive loading  
190    conditions with measurement of lateral and axial displacements, and three other discs were  
191    sealed with two layers of adhesive aluminum tape to ensure a one-dimensional gas flow  
192    through the discs. These specimens were oven-dried at 105 °C to constant weight before  
193    permeability testing was conducted using the Cembureau device.

194

Constituents (kg/m <sup>3</sup> )	OPC C1
Cement CEM I 52.5 N CE CP2 NF	240
Siliceous Sand 0/2 or 0/4	941
Siliceous aggregates 4-14 or 10-14	1019
Water	193
Superplasticizer	0.96
W/C	0.8
Slump (cm)	14

195

*Table 1: Mix proportions of concrete*

Properties	OPC C1
Dry apparent density (kg/m <sup>3</sup> )	2 222
Open porosity measured by water saturation method (%)	18.3
Cembureau apparent permeability with an injection pressure of 0.5 bars measured in dried specimen (10 <sup>-16</sup> m <sup>2</sup> ) (= K <sub>ref,C</sub> )	7.71

197 *Table 2: Physical and transport properties (average of three measurements)*

Mechanical properties (28 days)	OPC C1
compressive strength (MPa)	21.5
Modulus of elasticity (MPa)	24927
Poisson ratio	0.208

199 *Table 3: Mechanical properties at 28 days (average of three measurements)*201 

## 2.2 Carbonation procedure

202 The nine slabs intended for non-destructive testing were referenced as N or T (Table 4). After  
 203 exposure to carbonation, the slabs referenced N were stored in Nantes (France) and those  
 204 referenced T, in Toulouse.

205 After a 28-day residence time in water, the slabs were oven-dried at 80 °C until constant  
 206 weight was reached. The dry mass,  $W_d$ , was used to calculate the water content at time  $t$   
 207 (Equation 1), which, in turn, was used to calculate the degree of saturation at time  $t$  (Equation  
 208 2). At the end of the drying phase, the slabs were stored in laboratory conditions. The four  
 209 slabs referenced as 1 (C1-1-7N, C1-1-8N, C1-1-1T, C1-1-2T) were completely sealed with  
 210 two layers of adhesive aluminum tape to prevent carbonation. The slabs referenced C1-2N,  
 211 C1-3N, C1 4N, C1-2T, and C1-3T were sealed on five faces only, to ensure a one-  
 212 dimensional carbonation processing from one side of the slab only (50 cm x 25 cm). These  
 213 slabs were placed in a chamber at 20 °C, with a relative humidity of 65% and a CO<sub>2</sub> content  
 214 of 50% to accelerate the carbonation process. The core samples were extracted from the

215 specific sampling slab at the end of the curing phase and stored with the slabs in the  
216 laboratory. They were also placed in the carbonation chamber to monitor carbonation  
217 progress, just like the slabs. However, during this phase, the different core samples were  
218 regularly broken and immediately sprayed with the phenolphthalein color indicator so as to  
219 assess the carbonation depth at a given point of time. When the different desired carbonation  
220 depths had been reached on the control core samples, the slabs were removed from the  
221 chamber and immersed in water to stop carbonation and to ensure complete saturation of the  
222 slabs.

223 The real carbonation depths measured after completion of the whole experimental procedure  
224 using NDT techniques, are presented in Table 4.

225

<b>Slab reference</b>	<b>Expected carbonation depth (mm)</b>	<b>Measured carbonation depth <math>d_c</math> (mm) (cf. Figure 1)</b>
C1-1-7N	0	0
C1-1-8N	0	0
C1-2N	10	9.1
C1-3N	20	18.2
C1-4N	30	27.3
C1-1-1T	0	0
C1-1-2T	0	0
C1-2T	10	10.5
C1-3T	20	17

226

*Table 4: Expected and measured carbonation depths*

227

### 228 2.3 Experimental procedure

229 The operating method consisted in varying the slab water content in order to obtain  
230 permeability and resistivity correlation curves according to the saturation level. After  
231 saturation, different phases of drying were undertaken in order to achieve measurements with

232 targeted water contents corresponding to identical saturation levels for all the slabs. For that  
233 purpose, the slabs were placed in a drying oven at 80 °C and dried while their weight loss was  
234 monitored. It was assumed that the concrete was not modified at 80 °C, since ettringite is  
235 considered to dehydrate at a temperature higher than 80 °C [Zhou and Glasser 2001] and  
236 therefore would have remained almost stable at 80 °C. When the targeted mass was obtained  
237 and the drying phase completed, the slabs were hermetically sealed in airtight bags for forty  
238 days to balance the humidity level of the slabs and prevent natural carbonation. Their mass  
239 was measured regularly to leak-check the bags. Once the slabs were taken to be homogenized,  
240 the slab mass,  $W(t)$ , was measured again. Then, resistivity and permeability measurements  
241 were carried out. The water content was determined from Equation 1:

$$242 \quad w(t) = (W(t) - W_d) / W_d \quad (1)$$

243 where  $w(t)$  is the water content at time  $t$ ,  $W(t)$  is the mass of the slab at time  $t$  (kg) and  $W_d$  is  
244 the mass of the dried slab (kg).

245 The degree of saturation at time  $t$  is obtained from Equation 2 as:

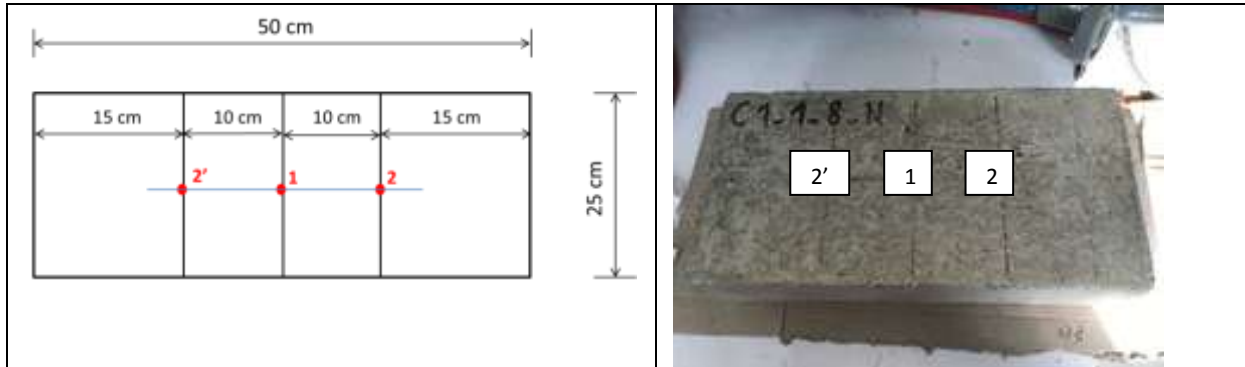
$$246 \quad S(t) = w(t) / w_{\text{sat}} \quad (2)$$

247 where  $w_{\text{sat}}$  is the water content of the saturated slabs.

248

249 For each measurement method (Wenner resistivimeter and Torrent permeameter), a total of  
250 ten measurements per test point and saturation level were performed. Measurements were  
251 carried out in the center of all the slabs (Point 1 in Figure 2). However, in order to check slab  
252 homogeneity and measurement sensitivity to side effects, measurements were also carried out  
253 on either side of Slab C1-1-8-N center (Points 2 and 2' in Figure 2). The measurements were  
254 made first at point 1, then at point 2 and finally at point 2' before returning to spot 1. So there  
255 was enough time between consecutive measurements in the same spot to allow vacuum  
256 dissipation.

257 The Wenner resistivity measurements were first carried out to determine the resistivity  
 258 values, which were afterwards used for the Torrent surface permeability measurements  
 259 [Torrent 1992].



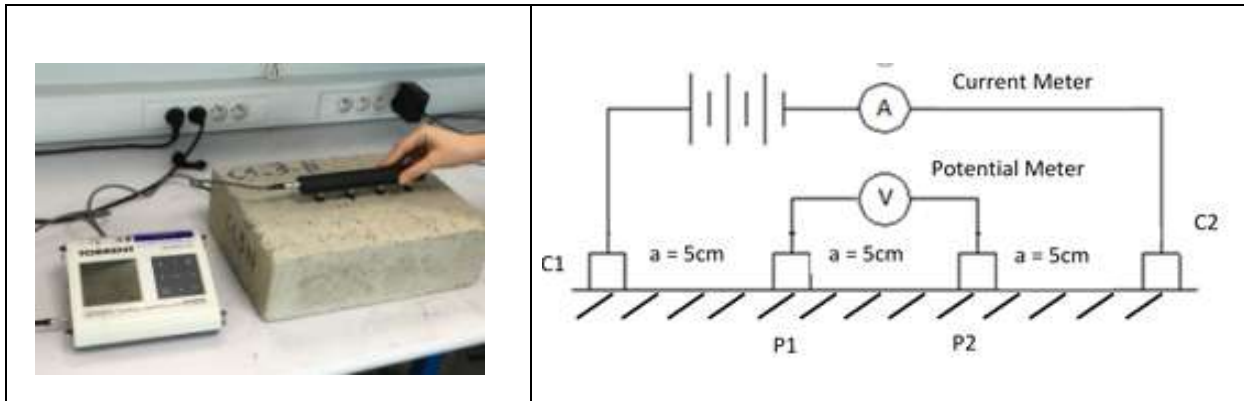
260 *Figure 2: Location of measurement points on the slabs*

261  
 262 The Wenner resistivimeter is a measurement device using Wenner protocol to determine the  
 263 apparent resistivity of concrete facings. Measurements are assumed to be carried out on a  
 264 semi-infinite homogeneous material. The measurement device is called a Wenner  
 265 resistivimeter because of the electrode arrangement, in which the distance interval between  
 266 the electrodes, called  $a$ , is the same, with  $a = \overline{C_1P_1} = \overline{P_1P_2} = \overline{P_2C_2}$  (Figure 3). The device used  
 267 in this work had a distance interval of 5 cm. First, an electric current,  $I$ , is injected between  
 268 electrodes  $C_1$  and  $C_2$ . Then, the electrical potential is measured between electrodes  $P_1$  and  
 269  $P_2$ . The apparent resistivity is calculated by the control acquisition unit, based on the  
 270 following formula:

271 
$$\rho = 2 \pi a \frac{V}{I} \quad (3)$$

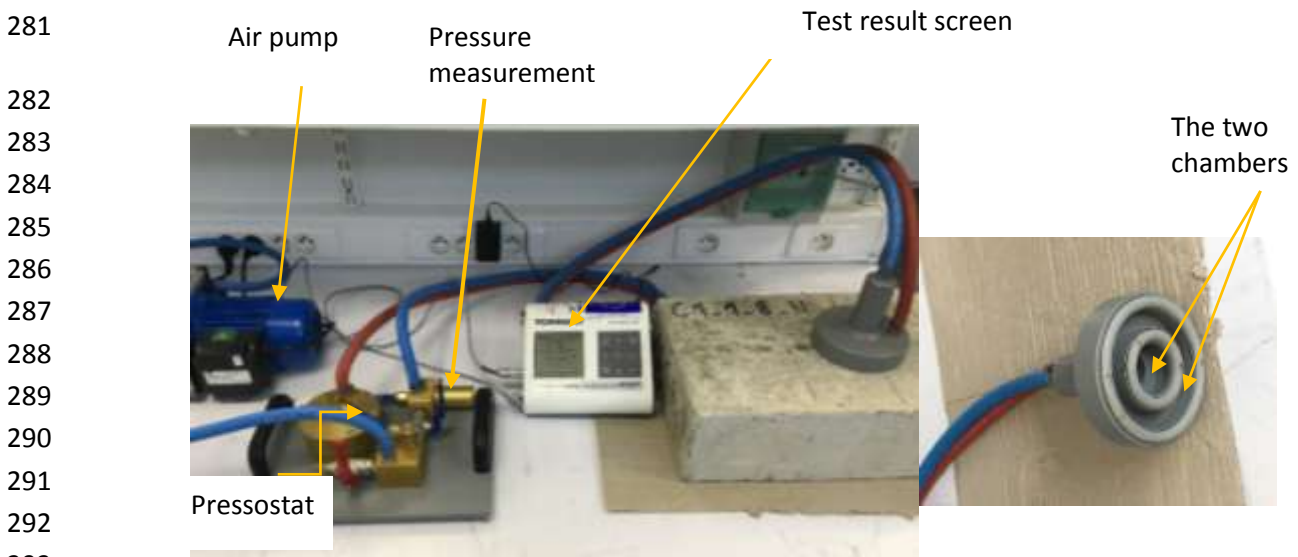
272 where  $\rho$  is the resistivity in  $\Omega.m$ ,  $a$  is the distance interval between the electrodes in  $m$ ,  $V$  is  
 273 the voltage in volts and  $I$  is the current intensity injected into the sample in amperes.

274



275 *Figure 3: Wenner resistivity measurements*

276  
 277 After the resistivity measurement was finished, the Torrent permeability was measured, if  
 278 possible, depending on the slab saturation level. The test principle is to create a vacuum inside  
 279 the test chamber using a vacuum pump and then disconnect the pump when the desired  
 280 pressure is reached (Figure 4).



281  
 282  
 283  
 284  
 285  
 286  
 287  
 288  
 289  
 290  
 291  
 292  
 293  
 294 *Figure 4: Torrent permeameter*

295  
 296 The rate of increase of pressure inside the vacuum cell can be measured and the air  
 297 permeability can be calculated according to the following formula:

$$298 \quad K = \left(\frac{V_c}{A}\right)^2 \cdot \frac{\mu}{2 \varepsilon P_a} \left[ \frac{\ln\left(\frac{P_a + \Delta P}{P_a - \Delta P}\right)}{\sqrt{t} - \sqrt{t_0}} \right]^2 \quad (4)$$

299

300 with:  $K$ : Torrent gas permeability coefficient ( $m^2$ ),  
301  $\mu$ : Air dynamic viscosity at 20 °C ( $2.0 \cdot 10^{-5}$  N.s/m<sup>2</sup>),  
302  $V_c$ : Capacity of the inner chamber and of the elements, through which air flows during  
303 the filling phase ( $V_c = 222 \cdot 10^{-6}$  m<sup>3</sup>),  
304  $\varepsilon$ : Concrete porosity introduced in the data (18.3 %, cf. Table 2).  
305  $A$ : concrete cross-section where air flows in the vacuum cell ( $19.6 \cdot 10^{-4}$  m<sup>2</sup>),  
306  $\Delta P$ : Pressure difference in the inner chamber in N/m<sup>2</sup>,  
307  $P_a$ : Atmospheric pressure in N/m<sup>2</sup>,  
308  $t_0$ : Test start time (60 s),  
309  $t$ : Test duration (< 720 s).

310

### 311 3 Results

#### 312 3.1 Resistivity results

313 Resistivity measurements at the three points on a given slab showed little scatter in the results,  
314 indicating that the concrete was homogeneous over the whole slab volume. It was concluded  
315 that the saturation level of the slab was spatially homogeneous on the surface investigated.  
316 Moreover, resistivity values were not influenced by side effects. Consequently, only the  
317 average of the different measuring points appears in Figures 5 to 8. The standard deviations  
318 were calculated from thirty measurements (ten measurements for Point 1, ten measurements  
319 for Point 2 and ten measurements for Point 2').

320 For saturation levels below 41%, measurements proved impossible for the most carbonated  
321 slab because it was too dry to allow electricity to flow freely between the electrodes.

322 Whatever the carbonation depth reached, Figure 5, 6, 7 and 8 show a lower resistivity when  
323 the sample saturation level increases. The trend observed in Figures 6 and 7 for non-  
324 carbonated samples has been highlighted by many authors [Sbartai 2007, Saleem 1996, Lopez

1993]. When the saturation level decreases, the concrete liquid phase gradually changes to a discontinuous pattern that makes ion conduction more difficult. Resistivity values then increase sharply. In non-carbonated slabs, resistivity increases by a factor of six between saturated samples and samples with a 41% saturation level. This explains the non-linear behavior of the electrical resistivity in relation to the variations of concrete saturation levels. Carbonation depth also affects resistivity. For the same saturation level, resistivity increases because of concrete structural changes due to carbonation reactions. The decrease in porosity induced by carbonation increases the material compactness, resulting in a less prevalent liquid phase. The current then flows less freely and resistivity increases.

334

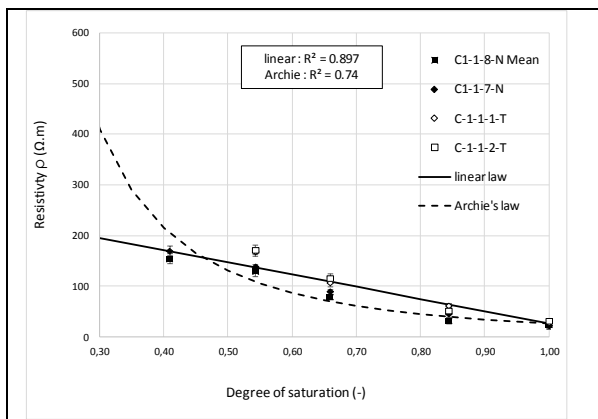


Figure 5: Resistivity versus saturation degree for non-carbonated slabs

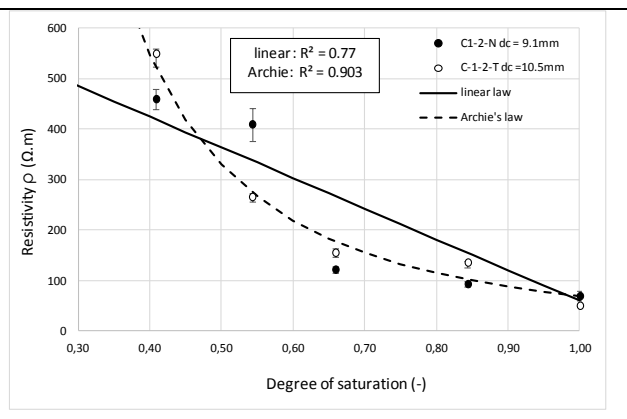


Figure 6: Resistivity versus saturation degree for carbonated slabs C1-2-N and C1-2-T ( $d_{cmean} = 9.8 \text{ mm}$ )

335

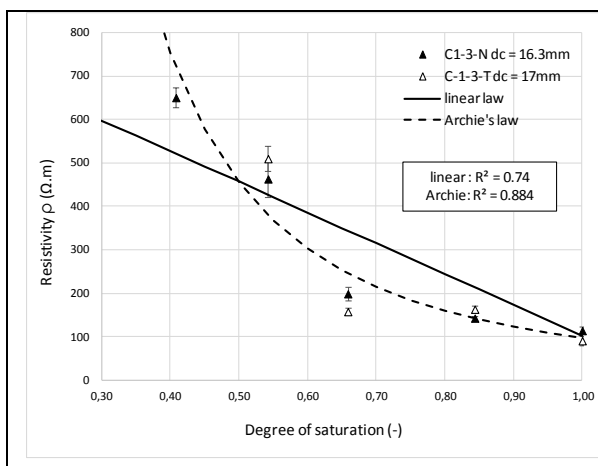


Figure 7: Resistivity versus saturation degree

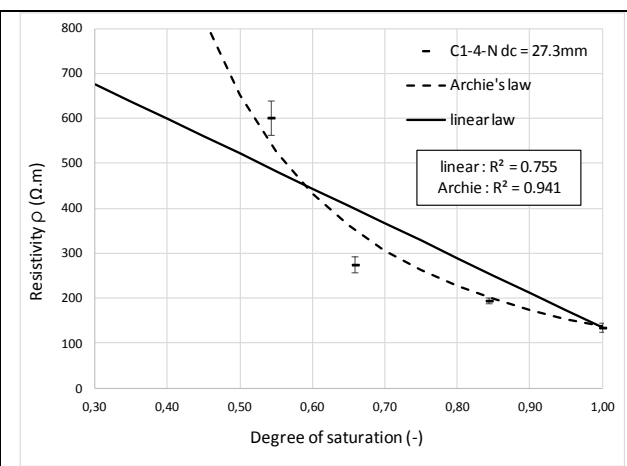


Figure 8: Resistivity versus saturation degree



<i>degree for carbonated slabs C1-3-N and C1-3-T (<math>d_{cmean} = 16.65 \text{ mm}</math>)</i>	<i>for carbonated slab C1-4-N with <math>d_c = 27.3 \text{ mm}</math></i>
--	---

336 Some mathematical laws are now examined for best fitting of the experimental points. We  
337 first select a linear law because the results achieved for the non-carbonated slabs, within the  
338 saturation level range for which measurements are possible, follow a linear trend. Then the  
339 linear equation to determine the mean resistivity of saturated slabs when the degree of  
340 saturation is 100% is taken as:

$$341 \quad \rho = a * (1 - S) + b \quad (5)$$

342

343 In the case of non-carbonated and fully saturated slabs, b is the reference value  $\rho_{ref}$ , called the  
344 reference resistivity. This value corresponds to the mean resistivity obtained on non-  
345 carbonated slabs in saturated conditions (C1-1-8-N, C1-1-7N, C1-1-1-T, C1-1-2-T). Here, the  
346 value of b is 27.627  $\Omega.m$ .

347 In the case of carbonated slabs, b is the mean resistivity calculated from the two saturated  
348 slabs ( $S=100\%$ ). For a carbonation depth of 27.3 mm, the value of b is obtained using Slab  
349 C1-4-N only. The values of a obtained by fitting the experimental data using Equation 5 are  
350 reported in Table 6.

351

352 The empirical Archie's law [Archie 1942] is also used to describe the general trend identified  
353 in these figures. This law describes the dependency of resistivity on the degree of saturation  
354 (S), porosity ( $\phi$ ) and resistivity of the composition pore solution ( $\rho_{sol}$ ) as:

$$355 \quad \rho = \rho_{sol} * S^{-n} \phi^{-m} \quad (6)$$

356 Parameters m and n are usually regressed over the experimental data.

357

358 To use this law, some parameters must be set. The pore solution resistivity is assumed to be  
359 constant throughout the carbonation process. However, it is reasonable to believe that the

360 change in the cement matrix due to the dissolution of the portlandite modifies the pore  
 361 solution and therefore its conductivity.

362 The conductivity of the pore solution ( $\sigma_{sol}=1/\rho_{sol}$ ) can be expressed as:

$$363 \quad \sigma_{sol} = \sigma_{wat} + \Sigma(C_i * \lambda_i) \quad (7)$$

364 where  $\sigma_{wat} = 10^{-5} \text{ S/m}$  , corresponding to the water conductivity as found in [Shi 2003]

365  $C_i$  ionic content (mol/m<sup>3</sup>)

366  $\lambda_i$  ionic molar conductivity (S.m<sup>2</sup>/mol)

367

368 The conductivity of the pore solution is assessed by combining data by Andersson et al.  
 369 [Andersson 1989] and Nguyen [2006] (Table 5). Two solution conductivities are calculated:  
 370  $\sigma_{sol} = 8.92 \text{ S/m}$  with the values by Nguyen and  $\sigma_{sol} = 6.41 \text{ S/m}$  with the values by  
 371 Andersson. Both these authors used very similar Portland cement but the mixes were  
 372 different. The mean value ( $\sigma_{sol} = 7.66 \text{ S/m}$ ) is used to calculate the resistivity of the pore  
 373 solution of the sample tested. This value is of the same order of magnitude as the values found  
 374 in the literature, although the literature values obviously depend on cement type and water to  
 375 cement ratios [Sanish 2013, Sant 2011, Neithalath 2006].

376

Ion	Ionic molar conductivity (mS.m <sup>2</sup> /mol)	Ionic content (mol/m <sup>3</sup> ) [Nguyen 2006]	Ionic content (mol/m <sup>3</sup> ) [Andersson 1989]
Na <sup>+</sup>	5,01	100	42.3
K <sup>+</sup>	7.35	272	161.1
Ca <sup>2+</sup>	11.9	2.6	2.2
Cl <sup>-</sup>	7.63	0.5	Not evaluated
OH <sup>-</sup>	19.86	321.4	251.2 (calculated using measured pH)

377 *Table 5: Values used to calculate the conductivity of the pore solution*

378

379 In order to determine the factor n, which is assumed to be constant for both carbonated and  
380 non-carbonated slabs, the data obtained on non-carbonated slabs are used. In this case, the  
381 factor m is calculated using Archie's law for S=100% ( $\rho_{ref} = \rho_{sol} * \phi^{-m_{ref}}$ ). We then have  
382  $m_{ref} = 3.153$  with  $\rho_{ref} = 27.627 \Omega.m$ . The factor n is therefore determined by fitting the  
383 experimental data of the non-carbonated slabs using Archie's law as:  $n = 2.24$  (Figure 5). For  
384 the carbonated slabs (Figures 6, 7 and 8), n is kept constant and only m is adjusted to achieve  
385 the best possible fitting with the experimental data because it is assumed to depend on the  
386 microstructure, which changes during carbonation.

387 Table 6 displays the different law parameters and determination coefficients obtained. Both  
388 laws can be used to represent the trend obtained because the determination coefficients are  
389 correct in both cases. The determination coefficients given by the linear law, however, are  
390 lower, except on non-carbonated slabs, as the linear law does not represent points obtained for  
391 low saturation levels very accurately. It seems likely that, for a dry material, resistivity tends  
392 toward a very high value. This trend is thus best represented by Archie's law.

393

		a/n	b/m	Determination coefficient R <sup>2</sup>
Non-carbonated slabs	Linear	238.16	27.627	0.897
	Archie	2.24	3.153	0.74
$d_c \text{ mean} = 9.8 \text{ mm}$	Linear	725.955	59.9	0.77
	Archie	2.24	3.70	0.903
$d_c \text{ mean} = 16.65 \text{ mm}$	Linear	864.852	102.63	0.74
	Archie	2.24	3.89	0.884
$d_c = 27.3 \text{ mm}$	Linear	913.16	135	0.755
	Archie	2.24	4.10	0.941

394 *Table 6: a and b (linear law), n and m (Archie's law) and corresponding determination*  
395 *coefficient R<sup>2</sup>*

396

397 The relations of coefficients a and b with mean carbonation depth are described as a  
398 logarithmic function (Equation 8) with  $R^2 = 0.984$  and a linear function (Equation 9) with  $R^2$

399 = 0.982, respectively. As regards Archie's law, the plot of coefficient m versus mean  
400 carbonation depth is described by a linear function with  $R^2 = 0.91$  (Equation 10).

$$401 \quad a = 91.645 * \ln(d_c) + 442.03 \quad (8)$$

$$402 \quad b = 4.0198 * d_c + 27.627 \quad (9)$$

$$403 \quad m = 0.0389 * d_c + 3.153 \quad (10)$$

404 By combining relationships 5 and 6 with Equations 8, 9 and 10, we obtain the laws describing  
405 electrical resistivity versus carbonation depth and saturation degree, respectively (Equations  
406 11 and 12):

$$407 \quad \rho = (91.645 * \ln(d_c) + 442.03) * (1 - S) + (4.0198 * d_c + 27.627) \quad (11)$$

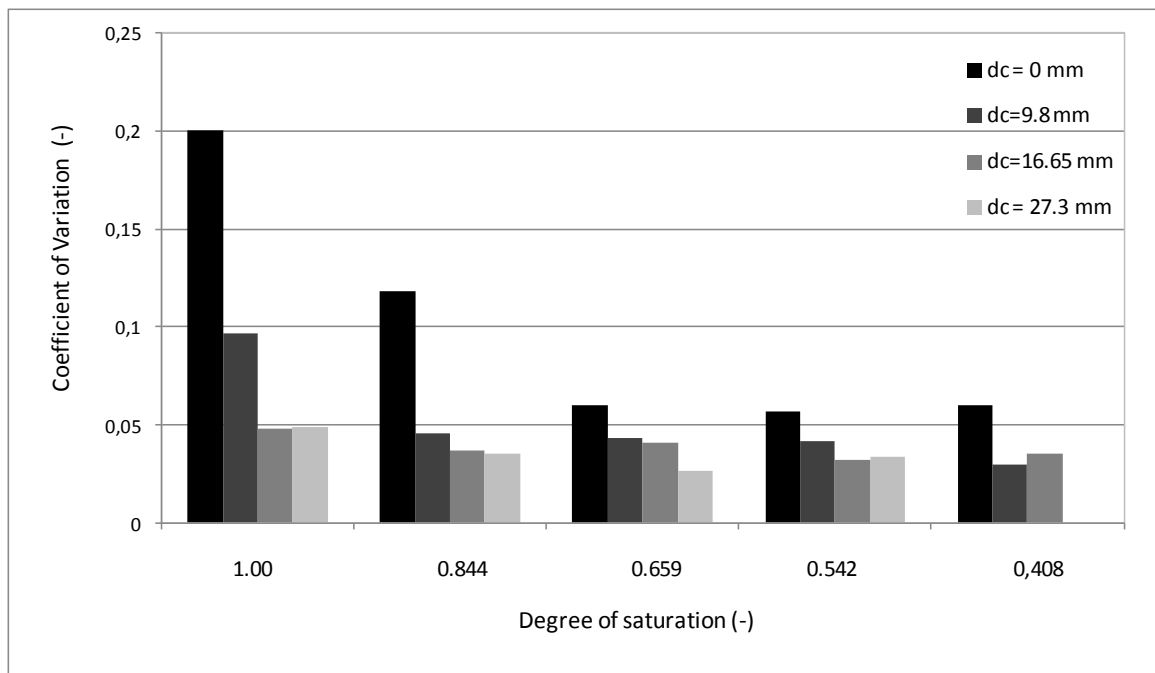
$$408 \quad \rho = \rho_{sol} * S^{-2.24} \phi^{-(0.0389*d_c+3.153)} \quad (12)$$

409 where  $d_c$  is the carbonation depth in mm and  $\rho$  the Wenner resistivity ( $\Omega.m$ )

410

411 The coefficients of determination obtained for the linear law parameters are higher than that  
412 obtained for parameter m of Archie's law. These laws may be used for the calculation of the  
413 saturation level from a resistivity measurement with knowledge of the carbonation depth. This  
414 depth would have been determined, for instance, by spraying phenolphthalein on a freshly  
415 drilled core sampled from the structure. Carbonation depth determination is faster than  
416 saturation level determination because it can be read immediately after sampling without  
417 waiting for the complete drying needed for saturation level measurements. However, the laws  
418 established here apply only to concrete with similar porosity (about 18%) and mixed with  
419 CEM I cement. Solution resistivity and carbonation process both depend on the type of  
420 cement and any addition modifies the chemical reactions. These laws should also consider the  
421 measurement error aspects. In order to seriously take the standard deviations displayed in  
422 [Figures 5, 6, 7 and 8](#) into account, [Figure 9](#) presents the Coefficient of Variation (CoV),

423 corresponding to the standard deviation divided by the average of the values measured, for all  
 424 the saturation levels. CoV values are very low (lower than 10% when the value obtained from  
 425 the saturation measurements carried out on the non-carbonated slabs is eliminated). Moreover,  
 426 this maximum value of 20% is of the same order of magnitude as the CoV calculated from  
 427 laboratory measurements (approximately 18%) [Ait-Mokhtar, 2013]. It may be recalled that  
 428 measurements appear reliable here, because the lower the CoV value, the higher the  
 429 measurement accuracy. The results obtained on the non-carbonated slabs correspond to the  
 430 lowest resistivity values and, hence, to higher CoV values. This analysis suggests that the  
 431 Wenner measurements carried out using this device can be reproduced.



432  
 433 **Figure 9:** Coefficient of variation of the resistivity measurements as a function of saturation  
 434 degree and carbonation depth

435  
 436 **3.2 Air permeability results**

437 **Permeability measurements at the three points on a given slab showed scatter in the results.**  
 438 **The differences observed cannot be attributed to the heterogeneity of the concrete material as**  
 439 **all the resistivity measurements performed on the same slab for a given saturation level are**

440 almost identical whatever the measurement point. Because side effects have not been  
441 demonstrated, the three point averages are presented with, on either side, the range defined by  
442 the standard deviation calculated from all the values (30 measurements). Moreover, on  
443 different concrete compositions, Neves *et al.* showed that, if the average of a set is used as the  
444 representative value, it is possible to distinguish between different concrete mixes and  
445 different curing (for the same mix) [Neves 2012].

446 Figures 10 through 13 show that, for a given carbonation depth, gas permeability decreases  
447 when the saturation level increases and also decreases when carbonation depth increases.  
448 Permeability also varies greatly in the slabs, which are supposed to be of the same concrete  
449 and in the same saturation state. Figure 10 shows that, when  $S_r = 15\%$ , permeability ranges  
450 from 17 to 25.10-16  $m^2$ , i.e. an increase of almost 50%. Although measurements are not  
451 possible on the fully saturated samples, they can, nevertheless, be performed up to 84%.  
452 Above this saturation rate, gas can no longer flow freely because of water molecule continuity  
453 in the concrete porous network. Concrete relative humidity reduces pore interconnectivity  
454 and, therefore, affects its permeability. The permeability vs. saturation level curve has already  
455 been assessed in the literature for non-carbonated materials using Cembureau measurements  
456 carried out on different concrete types [Kameche 2014, Abbas 1999]. These authors have  
457 established a logarithmic law to describe, as far as possible, the experimental results regarding  
458 intrinsic permeability as a function of saturation level for different sample sizes.  
459 Measurements are possible up to approximately 80% of the saturation level. As regards the  
460 work of Abbas *et al.* [Abbas 1999], a linear law best represents the results obtained for the  
461 apparent permeability measurements at different pressures as a function of the saturation  
462 level, with a saturation threshold of 90%. It should, however, be noted that the measurement  
463 variation ranges of both studies are larger than that obtained in the present paper using the  
464 Torrent permeameter, which results in a logarithmic display of their results. The present

465 results, on the other hand, are displayed on a linear scale for viewing comfort. They are fitted  
 466 with a linear law for all the carbonation depths reached by imposing zero permeability as a  
 467 condition for the saturated samples ( $S = 100\%$ ). This law is described by Equation 13. As  
 468 regards dry, non-carbonated slabs, the reference value,  $K_{ref,T}$  is imposed as the value for a.  
 469 This value corresponds to the average obtained from the Torrent permeability measurements  
 470 carried out on the dry non-carbonated Slabs C1-1-8-N, C1-1-7-N, C1-1-1-T and C1-1-2-T, is  
 471  $27.34 \cdot 10^{-16} \text{ m}^2$ .

$$472 \quad K = a * (1 - S) \quad (13)$$

473  
 474 The coefficients of determination are correct in view of the large standard deviations, which  
 475 make it possible to confirm that the linear laws express Torrent permeability evolution  
 476 satisfactorily as a function of the saturation level.

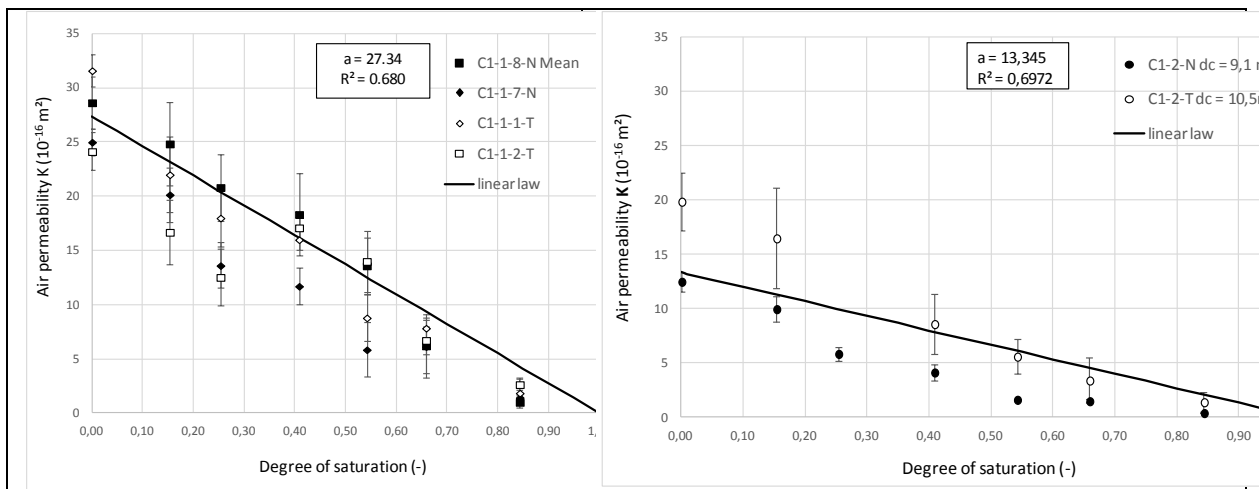


Figure 10: Torrent permeability versus saturation level for non-carbonated slabs

Figure 11: Torrent permeability versus saturation level for carbonated slabs C1-2-N et C1-2-T ( $d_{c \text{ mean}} = 9.8 \text{ mm}$ )

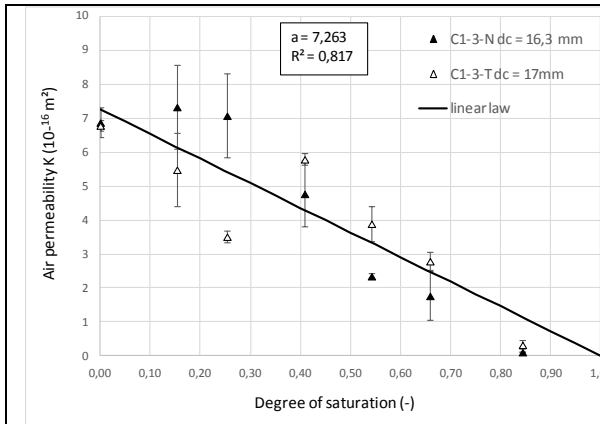


Figure 12: Torrent permeability versus saturation level for carbonated slabs C1-3-N et C1-3-T ( $d_{cmean} = 16.65$  mm)

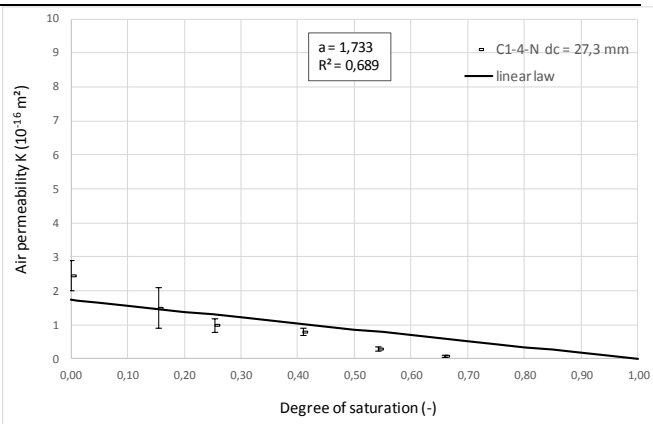


Figure 13: Torrent permeability versus saturation level for carbonated slabs C1-4-N ( $d_c = 27.3$  mm)

477 Equation 14 describes coefficient a versus carbonation depth and is then introduced into  
 478 Equation 15 to obtain Torrent permeability as a function of carbonation depth and saturation  
 479 degree. Law 14 is obtained with a good determination coefficient  $R^2 = 0.964$ . Both equations  
 480 take the form:

$$481 \quad a = 27.34 * e^{-0.0935*d_c} \quad (14)$$

$$482 \quad K = (27.34 * e^{-0.0935*d_c}) * (1 - S) \quad (15)$$

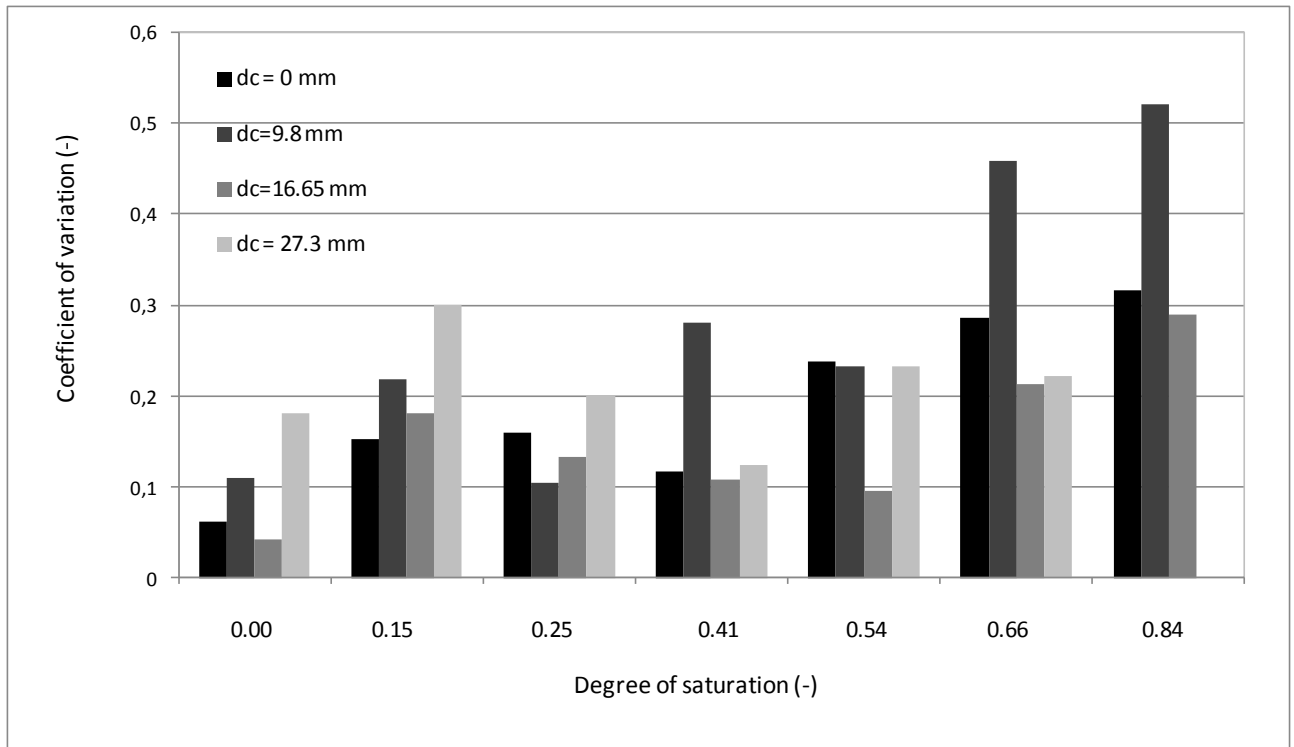
483 where  $d_c$  is the carbonation depth in mm and K is the Torrent measurement ( $10^{-16}$  m<sup>2</sup>)

484

485 This law (15) could be used to calculate the saturation level from a permeability measurement  
 486 with knowledge of the carbonation depth from phenolphthalein spraying on the fresh core  
 487 sampled from the concrete structure.

488 In view of Figures 10 through 13, standard deviation appears to decrease when saturation  
 489 level increases (only beyond a saturation level of 15%) to reach the lowest values for samples  
 490 with an 84% saturation level. However, this observation is surprising since permeability  
 491 measurements were conducted on completely dry samples, a condition required for correct  
 492 measurement of the gas permeability. So, the coefficients of variation according to the  
 493 saturation levels for the four carbonation depths studied are displayed in Figure 14.





494

495 *Figure 14: Coefficient of variation of Torrent permeability measurements as a function of*  
 496 *saturation degree and carbonation depth.*

497

498 The results presented in [Figure 14](#) are closer to expectations. Carbonation depth has no effect

499 on the measurements because trends observed in the carbonated slabs differ depending on the

500 saturation level. CoV, on the other hand, effectively increases with the degree of saturation. It

501 should be noted, however, that CoV could not be measured for  $d_c = 27.3$  mm at an 84.1%

502 saturation level, which was at the device operating limit. Moreover, with this saturation level,

503 the coefficient of variation ranges between 30 and 50%. This high range raises questions as to

504 measurement reliability. With these saturation levels, the device operating limits are

505 exceeded, all the more so when the concrete is compact. A key idea of this analysis is that

506 saturation level  $S$  and carbonation depth  $d_c$  can be determined from the measured  $K$  and  $\rho$  by

507 combining Equation 15 with Equation 11 or 12. However, these established relationships

508 apply only if the concrete porosity is equivalent (about 18%) and the formulation uses CEM I

509 cement, as in this study. Resistivity and permeability measurements depend on the material

510 composition, which in turn affects the porosity and conductivity of the pore solution.

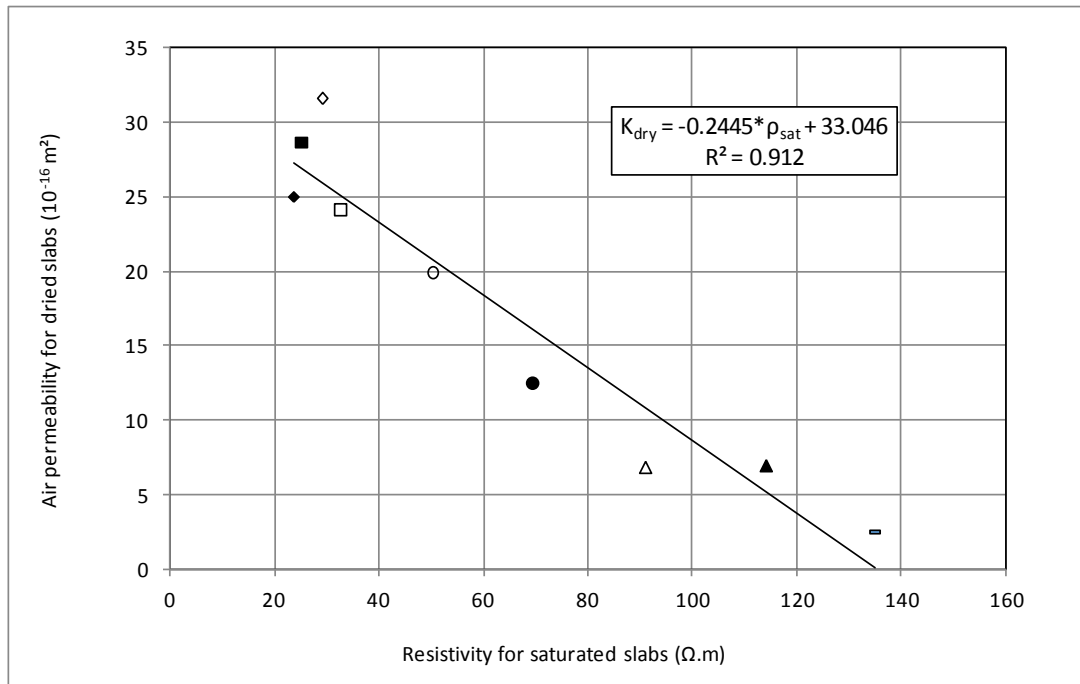
511 Moreover, the combination of the two laws is possible only if both measurements can be  
512 performed simultaneously, i.e., when the concrete saturation level falls within the range 40-83  
513 %, which is quite often the case where in situ concrete is concerned.

514

## 515 4 Result analysis

### 516 4.1 Correlation between resistivity and Torrent gas permeability

517 [Figure 15](#) shows the correlation between Torrent gas permeability measurements for dried  
518 slabs ( $S= 0\%$ ) and resistivity measurements carried out on saturated slabs ( $S = 100\%$ ). This  
519 comparison is possible since the saturation level is set aside as the impact of pore saturation is  
520 canceled out. The symbols used are the same as in [Figures 5 through 8 and 10 through 13](#). A  
521 linear correlation is observed between the two parameters. The slabs with the highest  
522 permeability present the lowest resistivity. Both properties share some crucial pore structure  
523 characteristics, such as total porosity, pore tortuosity and connectivity, of the cover concrete  
524 subjected to carbonation. They are sensitive to the different phases occurring within pores:  
525 gas permeability is linked with the characteristics of the gas phase and resistivity depends on  
526 the liquid phase through its electrochemical composition. Nevertheless, a good linear  
527 correlation is observed for the material studied here. The correlation established by Gui et al.  
528 [Gui 2016] for a study conducted to examine gas permeability using the Cembureau device  
529 and electrical conductivity using the high frequency alternating current method on laboratory  
530 concrete specimens with different water to binder ratios and different admixtures is not as  
531 good as the correlation proposed in this paper.



532

533 *Figure 15: Torrent permeability for dried slabs versus resistivity for saturated slabs*

534

535 4.2 Resistivity analysis

536 **Relative resistivity is considered because it could be useful to compare different concretes:** it

537 has been used by Gui et al. to study electrical conductivity and gas permeability of concrete

538 formulated with CEM I and blast-furnace slag cement [Gui, 2016]. Using a relative value for

539 resistivity and permeability could also be very useful for a modeling approach [Li, 2016].

540 Resistivity values are then processed after dividing them by the reference value  $\rho_{ref}$ . This

541 value can be considered as an intrinsic transport property since the impact of carbonation and

542 pore saturation is canceled out. This value is measured directly on the slabs using the Wenner

543 method. However, in future, taking the value measured on laboratory samples as the reference

544 value when selecting concrete type might be contemplated [Baroghel-Bouny, 2004; Aït-

545 Mokhtar, 2013].

546 We use the following relationship to fit the experimental data:

$$547 \quad \frac{\rho}{\rho_{ref}} = A * (1 - S) + B \quad (16)$$

548 with  $A=a/\rho_{ref}$  and  $B = b/\rho_{ref}$ , a and b being the values reported in Table 6.

549 Solutions are obtained from Equations 8 and 9 as:

$$550 \quad A = 3.317 * \ln(d_c) + 16 \quad (17)$$

$$551 \quad b = 0.1455 * d_c + 1 \quad (18)$$

552 Considering Archie's law, Equation 16 becomes:

$$553 \quad \frac{\rho}{\rho_{ref}} = S^{-n} \phi^{-(m-m_{ref})} \quad (19)$$

554 where  $n= 2.24$ ,  $m_{ref}$  corresponds to the value calculated in Section 3.1,  $m_{ref} = 3.153$ , and

555 values of  $m$  are given by Equation 10. We have:

$$556 \quad \frac{\rho}{\rho_{ref}} = (3.317 * \ln(d_c) + 16) * (1 - S) + (0.1455 * d_c + 1) \quad (20)$$

$$557 \quad \frac{\rho}{\rho_{ref}} = S^{-n} \phi^{-(m-m_{ref})} \quad (21)$$

558 where  $m = 0.0389 * d_c + 3.153$  and  $d_c$  is the carbonation depth in mm

559

560 [If these laws are validated with concretes presenting other porosities, they may be used for](#)  
561 [different concrete types if the  \$\rho\_{ref}\$  measurement is given.](#) This  $\rho_{ref}$  measurement value should  
562 become a durability indicator on which the choice between concretes for engineering  
563 structures could be based [\[Baroghel-Bouny, 2004\]](#).

564 These laws present equations with two unknown variables (saturation level and carbonation  
565 depth) whereas the survey of the structure provides only the resistivity  $\rho$ . Consequently, it is  
566 essential to combine this equation (linear or exponential) with the relationship established for  
567 permeability.

568

#### 569 4.3 Permeability analysis

570 In order to establish correlations that are independent of the permeability measured on dry,  
571 non-carbonated concrete, a relative permeability approach is used [\[Djerbi Tegguer 2013,](#)  
572 [Kameche 2014\]](#). Permeability values are then processed after being dividing by the reference  
573 value  $K_{ref,T}$ . This value, which is the average  $K$  value of the Torrent permeability measurements

574 on dry Slabs C1-1-8-N, C1-1-7-N, C1-1-1-T and C1-1-2-T, is  $27.34 \cdot 10^{-16} \text{ m}^2$ . The  
575 permeability measured on a sound, dry sample should become a mandatory parameter for  
576 selecting concrete mixtures. This value can be considered as an intrinsic transport property  
577 since the impact of carbonation and pore saturation is canceled out. This measurement value  
578 might become a durability indicator that could be provided with the formulation of concrete  
579 [Baroghel-Bouny 2004, Aït-Mokhtar 2013].

580 The results are displayed in [Figures 16 through 19](#) for different carbonation depths. They are  
581 fitted first with a linear law, then with a Van Genuchten law modified by Mualem [1976] and  
582 used by [Kameche 2014] to represent relative permeability as a function of saturation level.

583 When fitting with the linear law, the coefficients of determination achieved using Equation 15  
584 are obtained as:

$$585 \quad \frac{K}{K_{\text{ref,T}}} = e^{-0,0935 \cdot d_c} * (1 - S) \quad (22)$$

586 with  $d_c$  the carbonation depth in mm.

587 The modified Van Genuchten law (VG law) is then defined as:

$$588 \quad \frac{K}{K_{\text{ref,T}}} = (1 - S)^q * (1 - S^2) \quad (23)$$

589 Parameter  $q$  is determined by fitting this law with the experimental results obtained on non-  
590 carbonated slabs. The results displayed in [Figure 16](#) show that  $q = 0.89$ . This value is lower  
591 than the values previously achieved for cementitious materials. Monlouis-Bonnaire  
592 [Monlouis-Bonnaire 2004] proposes  $q = 5.5$  for cementitious materials and [Kameche 2014],  
593  $q = 3.5$  for relative gas permeabilites measured using the Cembureau method. Permeability  
594 variations are very pronounced when they are measured using the Torrent permeameter. For a  
595 40% saturation level, relative permeability is 0.6 with the Torrent method but only 0.1 with  
596 the Cembureau method [Kameche 2014]. Parameter  $q$ , used to quantify the effect of saturation  
597 level on relative permeability, is held constant for carbonated slabs. However, a  $C$  factor is  
598 introduced to consider the decrease in relative permeability with carbonation.

599

600 The VG law then becomes:

$$601 \quad \frac{K}{K_{ref,T}} = C * (1 - S)^q * (1 - S^2) \quad (24)$$

602 **Figure 20** presents the empirical parameter, C, determined by fitting with the experimental  
 603 results.

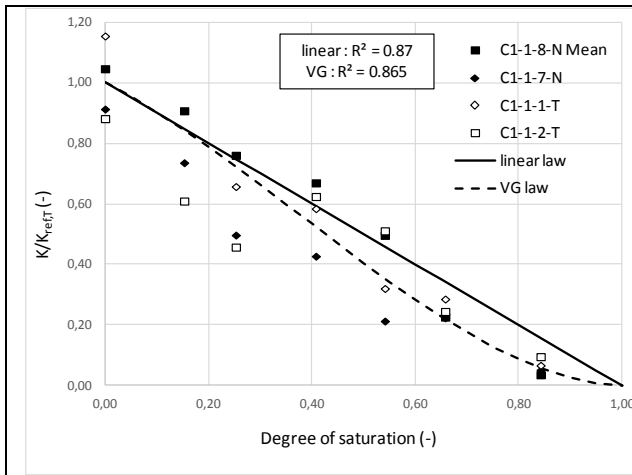


Figure 16: Relative permeability versus saturation degree for non-carbonated slabs

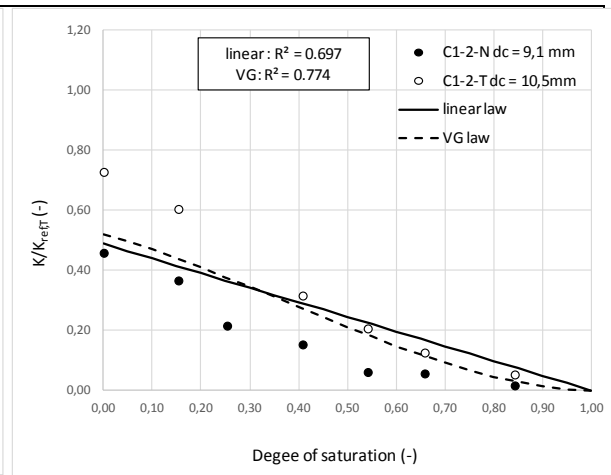


Figure 17: Relative permeability versus saturation degree for carbonated slabs C1-2-N et C1-2-T ( $d_c$  mean = 9.8 mm)

604

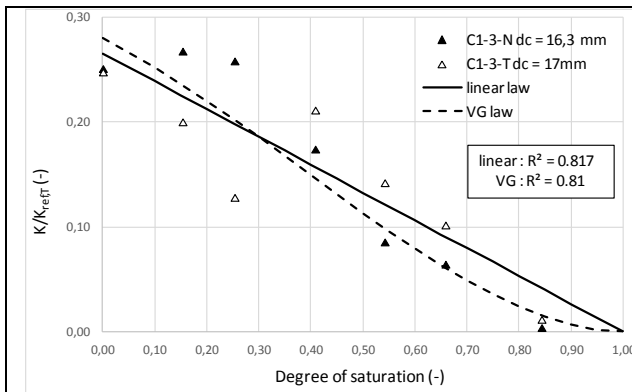


Figure 18: Relative permeability versus saturation degree for carbonated slabs C1-3-N et C1-3-T ( $d_c$  mean = 16.65 mm)

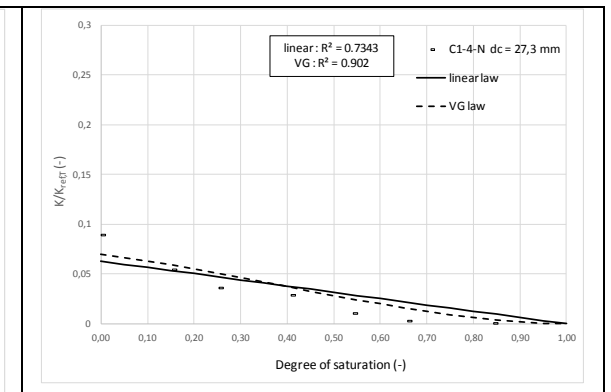
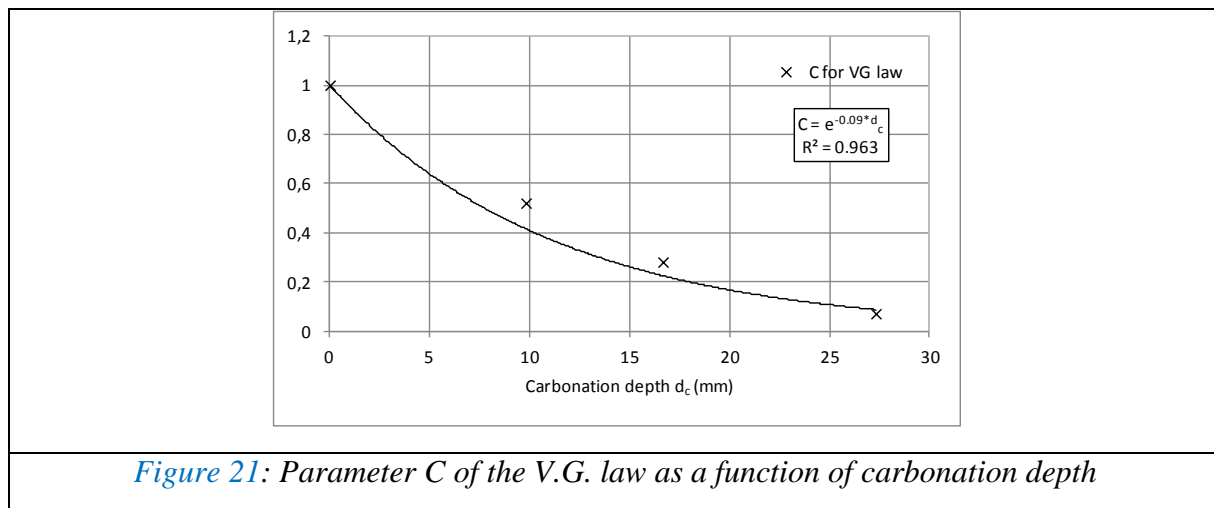


Figure 19 : relative permeability versus saturation degree for carbonated slabs C1-4-N ( $d_c = 27.3$  mm)

605



*Figure 21: Parameter C of the V.G. law as a function of carbonation depth*

606  
 607 The coefficients of determination demonstrate that the VG law describes relative permeability  
 608 evolution better. This law can therefore be used to describe Torrent permeability evolution  
 609 according to carbonation depth and saturation level as:

610

$$611 \quad \frac{K}{K_{\text{ref,T}}} = e^{-0.09*d_c} * (1 - S)^{0.89} * (1 - S^2) \quad (25)$$

612 with  $d_c$  the carbonation depth in mm.

613 The VG law for relative permeability and Archie's law for relative resistivity can be used to  
 614 obtain better coefficients of determination than with linear laws, in particular for carbonated  
 615 slabs. The two laws can be combined to determine the saturation level and the carbonation  
 616 depth of similar concrete structures. However, in order to use both measurement techniques  
 617 simultaneously, the concrete saturation level of the structure must fall within the range 40-  
 618 66%.

619 *If validated with concrete presenting other porosities, these laws may also be used on other*  
 620 *concrete materials if  $K_{\text{ref,T}}$  measurements, carried out using the Torrent permeameter on dry*  
 621 *non-carbonated samples, and  $\rho_{\text{ref}}$  measurements, carried out using the Wenner resistivimeter*  
 622 *on saturated non-carbonated samples, are given. Both measurements could be performed prior*  
 623 *to the construction in order to ensure the best choice of concrete formulations. During the*  
 624 *survey conducted to apply these laws, the surveyed areas of the structure should be checked*

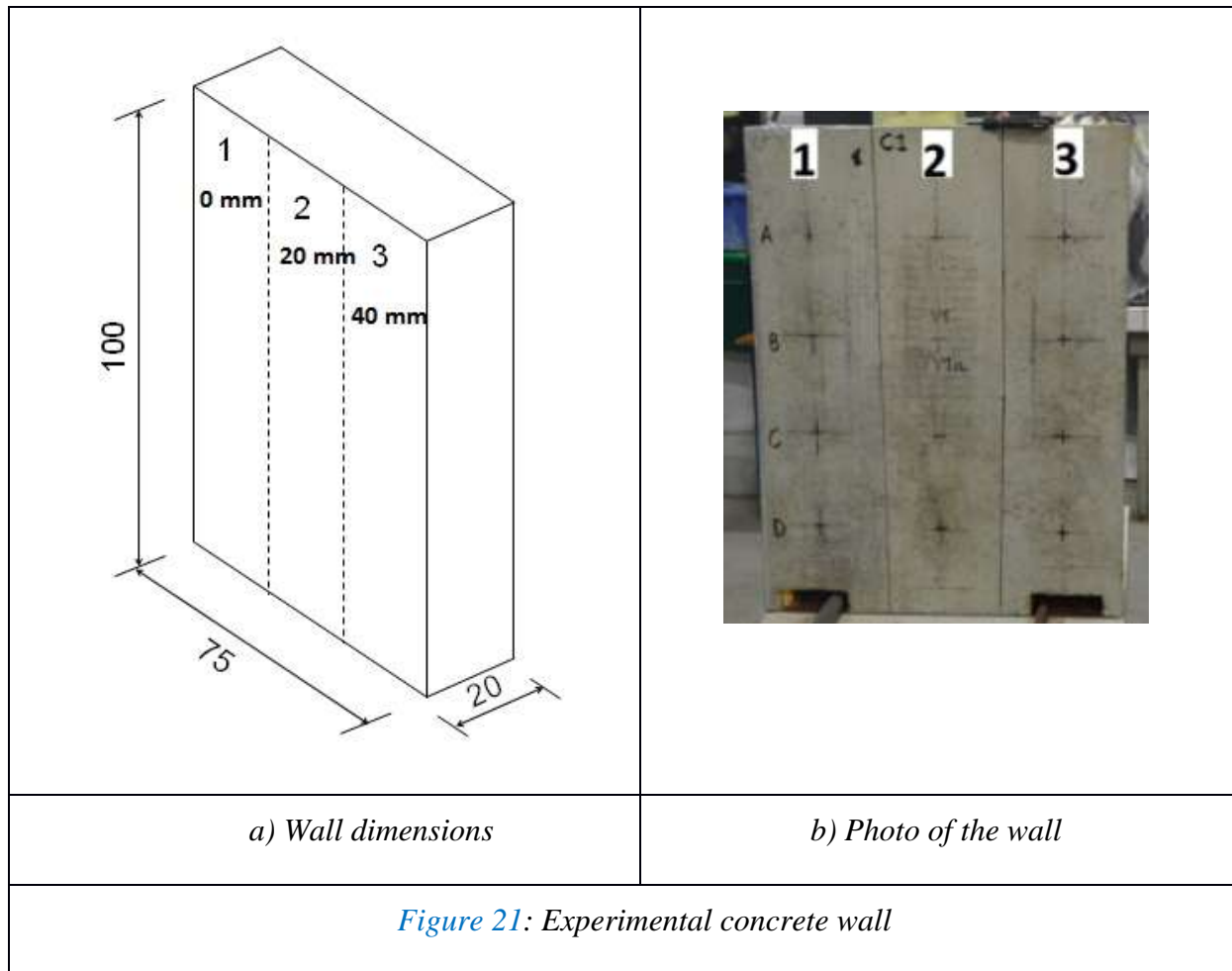
625 for cracking, as concrete damage modifies permeability [Picandet, 2001; Djerbi, 2008 and  
626 2013] as well as resistivity measurements [Taillet, 2014; Lataste 2003]. If damage is detected,  
627 another non-destructive technique should be used and relationships between, for instance,  
628 resistivity measurement and saturation level, carbonation depth and damage should be  
629 established.

630

#### 631 4.4 Validation using a concrete wall

632 The slabs studied in this paper were used to examine the influence of carbonation on NDT  
633 measurements by studying moisture homogeneity on saturated or partially saturated concrete.  
634 Equations 11, 12 and 15 were established using experimental measurements carried out on the  
635 slabs. In order to validate the performance of these laws, an experimental wall, 100 cm x 75  
636 cm and 20 cm thick, was prepared (Figure 21a). The concrete used for the wall was the same  
637 as for the slabs. A reinforcement mesh was placed at a depth of 25 mm on one face of the  
638 wall. The diameter of the bars was 10 mm and the size of square mesh was 20 cm.  
639 Measurements were only made on the non-reinforced side of the wall in order to avoid the  
640 influence of the reinforcement, especially on resistivity measurements. This face of the wall  
641 was divided into three vertical sections corresponding to different carbonation depths. After  
642 28 days of storage in a humid chamber, the first section (noted 1 in Figure 21), corresponding  
643 to a carbonation depth of 0 mm, was completely sealed. Then, the wall was placed in a  
644 carbonation chamber at 20 °C and 65% relative humidity, with a CO<sub>2</sub> content of 50% to  
645 accelerate the carbonation process. Section 2, corresponding to a carbonation depth of 20 mm,  
646 was also sealed after the same exposure to the carbonation process as Slabs C1-3N and C1-  
647 3T. The wall was finally removed from the carbonation chamber after the same exposure time  
648 as Slab C1-4N.





649

650 NDT measurements were carried out at twelve points on the wall (indicated with crosses in

651 [Figure 21b](#)). Then, core samples were taken in the center of each mesh to obtain real

652 carbonation depths and saturation levels. Each core sample was cut into three pieces: one

653 from each end, with a thickness corresponding to the desired carbonated depth, and one

654 middle piece corresponding to sound concrete (non-carbonated). [Because coring and sawing](#)

655 [were done under water, at the end of the operations, samples were dried with a cloth to avoid](#)

656 [the absorption of water as far as possible and so to avoid modifying the moisture content.](#) The

657 carbonation depth was observed by spraying the core samples with the phenolphthalein color

658 indicator and the saturation level was calculated after drying the core samples as described in

659 Section 2.3. The values reported in Table 7 are the mean values obtained from 8

660 measurements (four core samples for each vertical section and two pieces for each core  
661 sample).

Vertical section	Measured carbonation depth (mm)	Measured saturation level (%)	Mean permeability $10^{-16} \text{ m}^2$	Mean Wenner resistivity $\Omega \cdot \text{m}$	Calculated carbonation depth (mm)		Calculated saturation level (%)	
					equations 11 + 15	equations 12 + 15	equations 11 + 15	equations 12 + 15
1	0.25	65	1.7	22	0.003	0	93.7	93.7
2	18.9	58.9	1.07	407	24.4	24.38	61.7	61.8
3	33.1	60.6	0.101	504	48.8	38.9	64.9	86

662 *Table 7: Comparison between measured and calculated values of carbonation depth and*  
663 *saturation level.*

664  
665 In Section 1, Torrent permeability measurements were carried out with a saturation level that  
666 was considered high for such a measuring technique. As shown in [Figure 14](#), CoV increased  
667 with the degree of saturation. This can explain the high calculated degree of saturation  
668 obtained in Section 1 in both cases (Equations 11+15 and 12+15). As regards the carbonated  
669 sections, the calculated values for carbonation depth were [overestimated](#) by non-destructive  
670 testing, which provides a safety margin regarding the service life assessment of concrete  
671 structures but can be expensive for owners because repair will take place earlier. The  
672 combination of Equations 12 and 15 is more consistent with the measured data especially as  
673 regards carbonation depth. This combination is recommended for carbonation depth  
674 calculations, while the combination of Equations 11 and 15 is advised for calculating the  
675 saturation level after testing concrete structures using the Wenner resistivimeter and the  
676 Torrent permeameter.

677  
678 **5 Conclusion**

679 In this study, resistivity and permeability measurements were performed on carbonated slabs  
680 conditioned at different saturation degrees. The results confirm that resistivity and  
681 permeability are both very sensitive to concrete moisture. They also clearly show that

682 carbonation affects resistivity and permeability. The higher the carbonated depth is, the higher  
683 is the resistivity and the lower is the permeability. This can be related to the reaction of  
684 carbonation, which decreases porosity. Resistivity cannot be assessed for water saturation  
685 degrees of less than 40% because, at such low moisture content, the continuity of the  
686 interstitial solution vanishes and the electrical current cannot circulate. On the other hand,  
687 permeability cannot be measured for saturation degrees higher than 83% due to the  
688 obstruction of pores by the interstitial solution, which prevents gas penetration. An analysis of  
689 the test results has shown a coefficient of variation of 20% for resistivity and less than 30%  
690 for permeability, which increases with the increase of saturation degree whatever the  
691 carbonated depth.

692 Two empirical laws have been proposed here to model resistivity measurements versus  
693 carbonated depth and saturation degree. The first one is adapted from a linear law between  
694 resistivity and saturation degree to take the carbonated depth into account. For the second one,  
695 Archie's law is adapted to take carbonation into account. The coefficient of determination is  
696 better for the linear model, which is easier to determine. In the same way, a linear model  
697 between permeability coefficient and saturation degree is extended to take the carbonated  
698 depth into account with a good determination coefficient.

699 Models involving relative resistivity and relative permeability have also been proposed. For  
700 resistivity, both the linear and Archie's law are considered. For permeability modeling, a  
701 modified Van Genuchten law seems more efficient than the modified linear model. [It would  
702 be interesting to check these models with concrete presenting other porosities.](#)

703 Finally, the different models have been used to predict both saturation degree and carbonated  
704 depth on a wall made with the same concrete as the slabs. The results show that the models  
705 are able to distinguish different carbonated depths but the assessment precision needs to be  
706 improved. Additional research is required, in particular to take the presence of cracks into

707 consideration. These may due to shrinkage or to mechanical effects, for instance, which have  
708 a significant influence on measurements. In order to improve the quality of the investigation,  
709 a third technique could be proposed, such as ultrasonic surface waves, which are able to  
710 investigate the cover concrete.

711

712

## 713 6 Acknowledgment

714 The French National Research Agency (ANR “Building and Sustainable Cities”) is gratefully  
715 acknowledged for supporting the ANR EvaDéOS project. [Our thanks are extended to Susan](#)  
716 [Becker, a native English speaker, commissioned to proofread the final English version of this](#)  
717 [paper.](#)

718

## 719 7 References

720 [Aït-Mokhtar 2013] Aït-Mokhtar A., Belarbi R., Benboudjema F., Burlion N., Capra B.,  
721 Carcassès M., Colliat J.-B., Cussigh F., Deby F., Jacquemot F., De Larrard T., Lataste J.-F.,  
722 Le Bescop P., Pierre M., Poyet S., Rougeau P., Rougelot T., Sellier A., Séménadisse J.,  
723 Torrenti J.-M., Trabelsi A., Turcry P., Yanez-Godoy H., Experimental investigation of the  
724 variability of concrete durability properties, *Cement and Concrete Research* 45 (2013) 21–36.

725 [Abbas 1999] Abbas A., Carcasses M., Ollivier J.P., Gas permeability of concrete in relation  
726 to its degree of saturation, *Materials and Structures*, Vol. 32, January-February 1999, pp 3-8.

727 [Andersson 1989] Andersson K., Allard B , Bengtsson M., Magnusson B., chemical  
728 composition of cement pore solutions, *cement and concrete research*, Vol. 19, pp. 327-332,  
729 1989.

730 [[Archie 1942](#)] [Archie G.E., The electrical resistivity log as an aid in determining some](#)  
731 [reservoir characteristics, \*Transaction of AIME\*, 1942, 146, pp.54-62](#)

732 [Baroghel-Bouny 2004] Baroghel-Bouny, V., “Concrete design for structures with predefined  
733 service life – durability control with respect to reinforcement corrosion and alkali–silica  
734 reaction state-of-the-art and guide for the implementation of a performance-type and  
735 predictive approach based upon durability indicators.” English version of Documents  
736 Scientifiques et Techniques de l’AFGC (Civil Engineering French Association), 2004.

737 [Bungey 2006] Bungey J., Millard S., Grantham M., *Testing of Concrete in Structures*, 4th  
738 Edition, Taylor and Francis Editors, 2006.

739 [Auroy 2015] Auroy M., Poyet S., Le Bescop P., Torrenti J.M., Charpentier T., Moskura M.,  
740 Bourbon X., Impact of carbonation on unsaturated water transport properties of cement-based  
741 materials, *Cement and Concrete Research*, Volume 74, August 2015, Pages 44-58.

742 [Breyse 2017] D. Breyse, J.-P. Balayssac, S. Biondi, A. Borosnyói, E. Candigliota, L.  
743 Chiauuzzi, V. Garnier, M. Grantham, O. Gunes, V. Luprano, A. Masi, V. Pfister, Z.M. Sbartai,  
744 K. Szilagyi, M. Fontan, Non Destructive Assessment of In-situ Concrete Strength:  
745 comparison of approaches through an international benchmark, *Materials and Structures*, Vol.  
746 50, N°133, 2017

747 [Chang 2004] Chang J.J., Yeih W., Huang R., Chen C.T., Suitability of several current used  
748 concrete durability indices on evaluating the corrosion hazard for carbonated concrete, *Mater.*  
749 *Chem. Phys.*, vol. 84, n° 1, p. 71-78, March 2004.

750 [Chang 2006] Chang C.F., Chen J.W., The experimental investigation of concrete carbonation  
751 depth, *Cement and Concrete Research* 36 (2006) 1760– 1767.

752 [Djerbi 2008] Djerbi A., Bonnet S., Khelidj A., Baroghel-Bouny V., Influence of traversing  
753 crack on chloride diffusion into concrete, *Cement and Concrete Research* 38 (2008) 877–883.

754 [Djerbi Tegguer 2013] Djerbi Tegguer A., A., Bonnet S., Khelidj A., Baroghel-Bouny V.,  
755 Effect of uniaxial compressive loading on gas permeability and chloride diffusion coefficient  
756 of concrete and their relationship, *Cement and Concrete Research* 52 (2013) 131–139.

757 [Du Ploy 2015] Du Plooy R., Villain G., Palma Lopes S., Ihamouten A., Dérobert X.,  
758 Thauvin B., Electromagnetic non-destructive evaluation techniques for the monitoring of  
759 water and chloride ingress into concrete: a comparative study, *Materials and structures* 48  
760 (2015) 369-386.

761 [Fares 2018] Fares M., Villain G., Bonnet S., Palma Lopes S., Thauvin B., Thierry M.,  
762 Determining chloride content profiles in concrete using a resistivity probe, submitted to  
763 *Cement and concrete Composites* in September 2017.

764 [Gui 2016] Gui Q., Qin M., Li K., Gas permeability and electrical conductivity of structural  
765 concretes: Impact of pore structure and pore saturation, *Cement and Concrete Research* 89  
766 (2016) 109–119.

767 [Houst 1983] Houst Y.F., Roelfstra P. E., Wittmann F.H., A model to predict service life of  
768 concrete structures, *Mater. Sci. Restor.*, p. 181-186, 1983.

769 [Hui-Sheng 2009] Hui-Sheng S., Bi-Wan X., Xiao-Chen Z., Influence of mineral admixtures  
770 on compressive strength, gas permeability and carbonation of high performance concrete,  
771 *Construction and Building Materials* 23 (2009) 1980-1985.

772 [Kameche 2014] Kameche Z.A., Ghomari F., Choinska M., Khelidj A., Assessment of liquid  
773 water and gas permeabilities of partially saturated ordinary concrete, *Construction and*  
774 *Building Materials* 65 (2014) 551–565.

775 [Lataste 2003] Lataste J.F., Sirieix C., Breyse D., Frappa M., Electrical resistivity  
776 measurement applied to cracking assessment on reinforced concrete structures in civil  
777 engineering, *NDT & E International*, Volume 36, Issue 6, September 2003, Pages 383-394

778 [Lecieux 2015] Lecieux Y., Schoefs F., Bonnet S., Lecieux T., Lopes S.P., Quantification and  
779 uncertainty analysis of a structural monitoring device: detection of chloride in concrete using  
780 DC electrical resistivity measurement, *Nondestructive Testing and Evaluation* 30(3) (2015)  
781 216-232.

782 [Li 2016] Li K., Stroeven M., Stroeven S., Sluys L.J., Investigation of liquid water and gas  
783 permeability of partially saturated cement paste by DEM approach, *Cement and Concrete*  
784 *Research* 83 (2016) 104–113.

785 [Lopez 1993] Lopez W., Gonzalez J.A., Influence of the degree of pore saturation on the  
786 resistivity of concrete and the corrosion of steel reinforcement, *Cement and Concrete*  
787 *Research*. Vol. 23 (1993) 368-376.

788 [Lübeck 2012] Lübeck A., Gastaldini A.L.G. , Barin D.S., Siqueira H.C., Compressive  
789 strength and electrical properties of concrete with white Portland cement and blast-furnace  
790 slag, *Cement and Concrete Composites*, Volume 34, Issue 3, March 2012, Pages 392–399.

791 [Monlouis-Bonnaire 2004] Monlouis-Bonnaire JP, Verdier J, Perrin B. Prediction of the  
792 relative permeability to gas flow of cement-based materials. *Cem Concr Res* 2004; 34:737–  
793 44.

794 [Mualem 1976] Mualem Y A new model for predicting the unsaturated hydraulic conductivity  
795 of porous media *Water Resour Res* 1976;12:513–22.

796 [Neithalath 2006] Neithalath N., Weiss J., Olek J., Characterizing Enhanced Porosity  
797 Concrete using electrical impedance to predict acoustic and hydraulic performance, *Cement*  
798 *and Concrete Research* 36 (2006), 2074–2085.

799 [Neves 2012] Neves R., Branco F., De Brito J., About the statistical interpretation of air  
800 permeability assessment results, *Materials and Structures* 45 (2012) 529–539.

801 [Neves 2015] Neves R., Sena Da Fonseca B., Branco F., Brito J., Castela A., Montemor M.F.,  
802 Assessing concrete carbonation resistance through air permeability measurements,  
803 *Construction and Building Materials* 82 (2015) 304-309

804 [Ngala 1997] Ngala V.T., Page C.L., Effects of carbonation on pore structure and diffusional  
805 properties of hydrated cement pastes, *Cem. Concr. Res.* 27 (1997) 995–1007.

806 [Nguyen 2006] Nguyen T.S., Influence of binder and temperature on the chloride transport in  
807 cementitious materials, PhD thesis, LMDC Toulouse France, (September 2006), in French.

808 [Nguyen 2017] [Estimation of reinforcement electrochemical state in water-saturated](#)  
809 [reinforced concrete by resistivity measurement](#), *Construction and Building Materials*, Vol.  
810 [171](#), May 2018, Pages 455-466

811 [Papadakis 1989] Papadakis V.G. , A reaction engineering approach to the problem of  
812 concrete carbonation, *AIChE J.*, vol. 35, n° 10, p. 1639–1650, 1989.

813 [Papadakis 1999] Papadakis V.G., Effect of fly ash on Portland cement systems: Part I. Low-  
814 calcium fly ash, *Cem. Concr. Res.*, vol. 29, n° 11, p. 1727–1736, 1999.

815 [Papadakis 2000] Papadakis V.G., Effect of fly ash on Portland cement systems: Part II. High-  
816 calcium fly ash, *Cem. Concr. Res.*, vol. 30, n° 10, p. 1647–1654, 2000.

817 [Picandet 2001] Picandet V., Khelidj A., Bastian G., Effect of axial compressive damage on  
818 gas permeability of ordinary and high-performance concrete, *Cement and Concrete Research*  
819 31 (2001) 1525–1532.

820 [Polder 2001] Polder R., Test methods for on site measurement of resistivity of concrete – a  
821 RILEM TC-154 Technical Recommendation, *Construction Building Materials* 15 (2001) pp.  
822 125–31.

823 [RILEM CPC-18] RILEM CPC-18, RILEM Committee, Measurement of hardened concrete  
824 carbonation depth, *Mater. Struct.* 18 (1988) 453–455.

825 [Romer 2005] Romer M., Effect of moisture and concrete composition on the Torrent  
826 permeability measurement, *Materials and Structures* 38 (June 2005) 541-547.

827 [Saetta 1993] Saetta A.V., The carbonation of concrete and the mechanism of moisture, heat  
828 and carbon dioxide flow through porous materials, *Cem. Concr. Res.*, vol. 23, p. 761-772,  
829 1993.

830 [Saleem 1996] Saleem M., Shameem M., Hussain S.E., Maslehuddintf M., Effect of  
831 moisture, chloride and sulphate contamination on the electrical resistivity of Portland cement  
832 concrete, *Construction and Building Materials*, Vol. 10, No. 3, (1996) 209-214.

833 [Sanish 2013] Sanish K.B., Neithalath N., Santhanam M., Monitoring the evolution of  
834 material structure in cement pastes and concretes using electrical property measurements,  
835 *Construction and Building Materials*, Volume 49, December 2013, Pages 288-297

836 [Sant 2011] Sant G., Bentz D., Weiss J., Capillary porosity depercolation in cement-based  
837 materials: Measurement techniques and factors which influence their interpretation, *Cement  
838 and Concrete Research* 41 (2011) 854–864.

839 [Sena da Fonseca 2015] Sena da Fonseca B., Castela A.S., Duarte R.G., Neves R., Montemor  
840 M. F., Non-destructive and on site method to assess the air- permeability in dimension stones  
841 and its relationship with other transport-related properties, *Materials and Structures* (2015) vol  
842 48, 3795–3809, DOI 10.1617/s11527-014-0440-2

843 [Sbartai 2007] Sbartai Z.M., Laurens S., Rhazi J., Balayssac J.P., Arliguie G., Using radar  
844 direct wave for concrete condition assessment: Correlation with electrical resistivity, *Journal  
845 of Applied Geophysics* 62 (2007) 361–374

846 [Shi 2004] Shi C., Effect of mixing proportions of concrete on its electrical conductivity and  
847 the rapid chloride permeability test (ASTM C1202 or ASSHTO T277) results, *Cement and  
848 Concrete Research* 34, pp 537–545, 2004.

849 [Ta 2016] Ta V.L, Bonnet S., Senga Kiese T., Ventura A., A new meta-model to calculate  
850 carbonation front depth within concrete structures, *Construction and Building Materials* 129  
851 (2016) 172–181

852 [Ta 2018] Ta V. L., Senga Kiese T., Bonnet S., Ventura A., Application of sensitivity  
853 analysis in the life cycle design for the durability of reinforced concrete structures in the case  
854 of XC4 exposure class, *Cement and Concrete Composites*, Volume 87, 2018, Pages 53–62,  
855 <https://doi.org/10.1016/j.cemconcomp.2017.11.024>.

856 [Taillet 2014] Taillet E., Lataste J.F., Rivard P., Denis A., Non-destructive evaluation of  
857 cracks in massive concrete using normal dc resistivity, *NDT & E International*, Volume 63,  
858 April 2014, Pages 11-20

859 [Torrent 1992] Torrent R.J., A two-chamber vacuum cell for measuring the coefficient of  
860 permeability to air of the concrete cover on site, *Materials and Structures* 25 (1992) 358-365.

861 [Villain 2001] Villain G., Baroghel-Bouny V. Hua C., Measuring the gas permeability as a  
862 function of saturation rate of concretes, *French J Civ Eng* 2001, [Transfer in concrete and  
863 durability, In French].

864 [Villain 2006] Villain G., Thiery M., Gammadensimetry: A method to determine drying and  
865 carbonation profiles in concrete, *NDT&E International* 39 (2006) 328–337.

866 [Younsi 2011] Younsi A., Turcry P., Rozière E., Ait-Mokhtar K., Loukili A., Performance-  
867 based design and carbonation of concrete with high fly ash content, *Cem. Concr. Compos.*,  
868 vol. 33, n° 10, p. 993-1000, nov. 2011.

869 [Zhou 2001] Zhou Q., F.P. Glasser F.P., Thermal stability and decomposition mechanisms of  
870 ettringite at <120°C, *Cement and Concrete Research*, vol. 31 (2001) 1333–1339.